Immunity, Vol. 22, 259–270, February, 2005, Copyright ©2005 by Elsevier Inc. DOI 10.1016/j.immuni.2005.01.008

# Bone Marrow Is a Major Reservoir and Site of Recruitment for Central Memory CD8+ T Cells

**Irina B. Mazo,[1] Marek Honczarenko,[2] Harry Leung,[1] Lois L. Cavanagh,[1,5] Roberto Bonasio,[1] Wolfgang Weninger,[1,5] Katharina Engelke,[1] Lijun Xia,[3] Rodger P. McEver,[3] Pandelakis A. Koni,[4] Leslie E. Silberstein,[2] and Ulrich H. von Andrian[1,*]**

[1]Department of Pathology
The CBR Institute for Biomedical Research
Harvard Medical School
Boston, Massachusetts 02215

[2]Joint Program in Transfusion Medicine
Children's Hospital
Harvard Medical School
Boston, Massachusetts 02215

[3]Oklahoma Medical Research Foundation
Oklahoma City, Oklahoma 73104

[4]Institute of Molecular Medicine and Genetics
Medical College of Georgia
Augusta, Georgia 30912

## Summary

**Normal bone marrow (BM) contains T cells whose function and origin are poorly understood. We observed that CD8+ T cells in BM consist chiefly of CCR7+ L-selectin+ central memory cells ($T_{CM}$s). Adoptively transferred $T_{CM}$s accumulated more efficiently in the BM than naive and effector T cells. Intravital microscopy (IVM) showed that $T_{CM}$s roll efficiently in BM microvessels via L-, P-, and E-selectin, whereas firm arrest required the VCAM-1/$\alpha4\beta1$ pathway. $\alpha4\beta1$ integrin activation did not depend on pertussis toxin (PTX)-sensitive G$\alpha$i proteins but was reduced by anti-CXCL12. In contrast, $T_{CM}$ diapedesis did not require CXCL12 but was blocked by PTX. After extravasation, $T_{CM}$s displayed agile movement within BM cavities, remained viable, and mounted potent antigen-specific recall responses for at least two months. Thus, the BM functions as a major reservoir for $T_{CM}$s by providing specific recruitment signals that act in sequence to mediate the constitutive recruitment of $T_{CM}$s from the blood.**

## Introduction

Although the importance of the BM in hematopoiesis is well known, its function in T cell-mediated immunity is only partly understood. Studies in mice have shown that the BM accumulates activated/memory T cells after exposure to environmental cognate antigens (Ags) (Price and Cerny, 1999) and promotes the long-term persistence of antiviral memory cells (Kuroda et al., 2000; Marshall et al., 2001; Slifka et al., 1997). In some circumstances, it can even support the priming of naive T cells (Feuerer et al., 2003; Tripp et al., 1997). BM-resident T cells are also important for BM transplantation (BMT) because contaminating T cells in BM allografts can cause graft versus host disease (GvHD). On the other hand, T cell depletion from allogenic BM grafts compromises engraftment (Martinez et al., 1999) because CD8+ (but not CD4+) T cells and dendritic cells (DCs) facilitate engraftment (Adams et al., 2003; Gandy et al., 1999; Zeng et al., 2002). Indeed, BM-resident T cells are functionally distinct from those in other compartments. Compared to their blood-derived cousins, BM-derived CD8+ T cells induce milder GvHD and tumor-specific cytotoxic lymphocytes (CTL) are more frequent and possess higher antitumor activity in BM than in blood of cancer patients (Feuerer et al., 2001a, 2001b; Zeng et al., 2002). Thus, the BM is being considered with growing interest as a source of T cells for cancer therapy (Schirrmacher et al., 2003).

Here, we asked how T cells accumulate in the BM and how they differ from T cells elsewhere. BM stroma cells can support lymphoid precursor cell differentiation into mature T cells in vitro (Garcia-Ojeda et al., 1998) and in athymic mice in vivo (Tsark et al., 2001). However, T cells in wild-type (wt) BM are probably immigrants from the blood because T cells are normally produced in the thymus. Indeed, the BM continuously recruits circulating hemopoietic stem cells (HSCs) (Wright et al., 2001) because BM microvessels constitutively express prerequisite traffic molecules (Mazo and von Andrian, 1999), which might also support homing of T cell subsets.

After exiting the thymus, naive T cells search for Ag by recirculating between blood and secondary lymphoid organs (SLOs). Upon Ag stimulation, T cells proliferate and become effector cells ($T_{Eff}$s); CD8+ $T_{Eff}$s produce cytokines, especially interferon (IFN)-$\gamma$, and become CTL. Upon Ag clearance most $T_{Eff}$s die, but a few give rise to memory cells providing long-term protection. Memory cells are subdivided into two subsets based on their migration pattern (Sallusto et al., 1999): effector memory cells ($T_{EM}$s) migrate to peripheral tissues to eliminate pathogens, whereas $T_{CM}$s express homing molecules, allowing them to migrate to SLOs, particularly lymph nodes (Weninger et al., 2001).

We show here that $T_{CM}$s constitute the largest endogenous subset of CD8+ T cells in murine BM and are also prominent in human BM. Accordingly, adoptively transferred $T_{CM}$s from immunized mice colonized recipient BM more effectively than $T_{EM}$s and naive T cells. The mechanisms by which in vivo-generated memory cell subsets are recruited to tissues have been difficult to study, because such studies require unattainable numbers of purified cells. We were able to circumvent this obstacle by using a recently described in vitro method to generate Ag-specific $T_{Eff}$s and $T_{CM}$s from TCR transgenic CD8+ T cells (Manjunath et al., 2001). After i.v. injection, naive T cells and $T_{CM}$s were more efficiently recruited to the BM than $T_{Eff}$s. Adoptively transferred $T_{CM}$s were much more efficiently retained in the BM than other subsets and mounted potent recall responses upon restimulation. By using IVM, we have

*Correspondence: uva@cbr.med.harvard.edu
[5]Present address: Wistar Institute, Philadelphia, Pennsylvania 19104.

dissected the multistep adhesion cascade for $T_{CM}$ recruitment to the BM and show that extravasated $T_{CM}$s move actively within BM cavities.

## Results

### $T_{CM}$s Are the Predominant Subset among CD8$^+$ T Cells in Murine BM

To investigate CD8$^+$ T cell traffic in normal BM, we compared the composition of CD8$^+$ T cells in BM, blood, and SLOs of adult mice. CD8$^+$ T cells comprised 2.5% ± 0.1% of all mononuclear cells (MNCs) in the BM, which is a much smaller fraction than in blood (7.9% ± 1.8%) or spleen (11.8% ± 0.1%; Figure 1A). Two-thirds of BM-resident T cells expressed surface markers indicative of Ag experience, i.e., they were CD44$^{hi}$ and CD122$^+$, whereas most CD8$^+$ T cells in spleen, peripheral lymph nodes (PLNs), and blood were naive (i.e., CD44$^{lo/-}$ CD122$^-$; Figure 1B). Thus, the BM differs from classic SLOs in terms of its accumulation of memory cells.

Memory T cells are subdivided based on their expression of CCR7 (Sallusto et al., 1999). $T_{CM}$s are CCR7$^+$ and mostly coexpress L-selectin. They home efficiently to PLN and other SLOs, whereas CCR7$^-$ $T_{Eff}$s and the longer-lived $T_{EM}$s are largely L-selectin$^-$ and accumulate in nonlymphoid tissues and to some degree in the spleen (Sallusto et al., 1999; Weninger et al., 2001). Thus, we examined CCR7 expression on CD44$^{hi}$ (memory) and CD44$^{lo}$ (naive) CD8$^+$ T cells by using CCL19-Ig chimera as a probe (Manjunath et al., 2001). As expected, naive T cells in all organs were CCR7$^+$ and L-selectin$^+$, whereas CD44$^{hi}$ T cells expressed these markers variably (Figure 1C). CCR7$^-$ $T_{EM}$s bound P-selectin (Table S1 available with this article online and data not shown) and represented approximately half of all memory cells in spleen and blood. By contrast, $T_{EM}$s were more sparse among BM CD8 cells where the largest subset was comprised of CCR7$^+$L-selectin$^+$ $T_{CM}$s that did not bind P-selectin. Consequently, although the spleen harbored many more naive CD8$^+$ T cells and $T_{EM}$s than the BM, the number of $T_{CM}$s was similar in both organs. Thus, mouse BM is a major reservoir for Ag-experienced CD8$^+$ T cells, most of which share a $T_{CM}$ phenotype.

We also examined CD3$^+$CD8$^+$ T cells in BM from healthy human donors by using mAbs specific for CCR7 and CD45RA (Sallusto et al., 1999). As shown in Figure 1D, naive T cells contributed only 21% of CD8$^+$ T cells, whereas the largest subsets (~30% each) were $T_{CM}$s (CD45RA$^-$CCR7$^+$) and $T_{EM}$s (CD45RA$^-$CCR7$^-$); a smaller fraction was comprised of $T_{Eff}$s (CD45RA$^+$CCR7$^-$). Similar results were obtained with two anti-CCR7 mAbs (clones 2H4 and 3D12), whereas a third anti-CCR7 mAb, 6B3 (Hasegawa et al., 2000), stained nearly 70% of CD45RA$^-$ CD8$^+$ T cells (not shown). Thus, mammalian BM is a rich source of $T_{CM}$s not only in mice kept in a pathogen-free facility but also in people.

### Preferential Homing and Retention of $T_{CM}$s in BM

The relatively larger proportion of CCR7$^-$ T cells in human versus murine BM might reflect the constant exposure to infectious Ags experienced in normal human life. To ask if this might also apply to mice, we transferred into wt recipients naive P14 CD8$^+$ T cells expressing a TCR for LCMV gp33–41 in H2-D$^b$. 1 day and again 3 weeks later, the mice received i.v. injections of mature peptide-pulsed DCs. After 5 more weeks, all CD8$^+$ T cells detected by a P14 TCR-specific MHC tetramer were CD44$^{high}$ in both BM and spleen. At least as many $T_{EM}$s as $T_{CM}$s were found in recipients' spleens, whereas $T_{CM}$s in BM outnumbered $T_{EM}$s. However, the $T_{CM}/T_{EM}$ ratio in BM after Ag challenge (1.8:1) was markedly re-

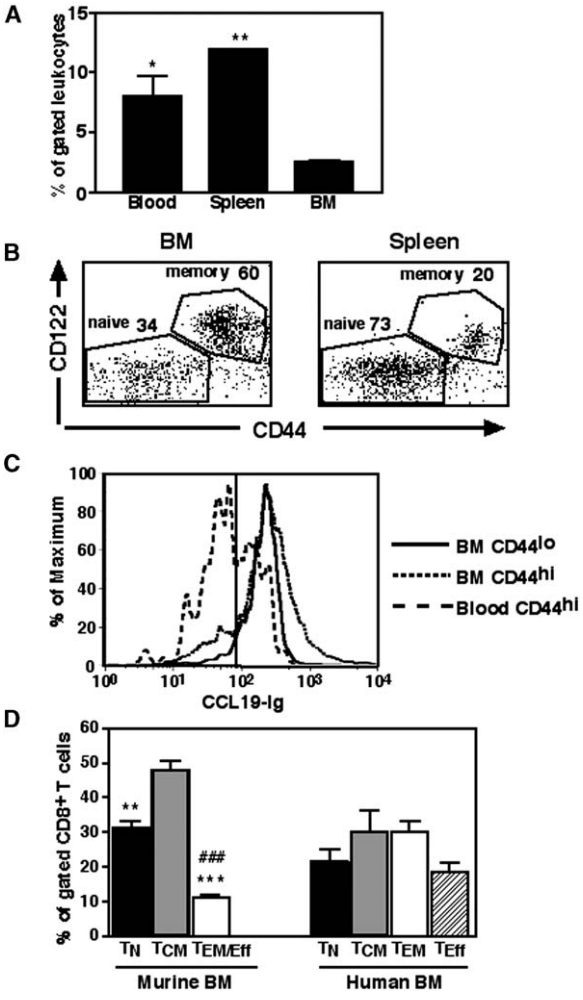


Figure 1. Subset Composition of Resident CD8$^+$ T Cells in Murine and Human BM

(A) The frequency of CD8β$^+$ cells in BM, spleen, and blood of young adult C57BL6 mice. *$p < 0.05$ and **$p < 0.01$ versus BM (one-way ANOVA). Error bars show mean ± SEM.

(B) Activation/memory markers on CD8β$^+$ T cells in mouse BM and spleen. Cell frequencies among all CD8β$^+$ T cells are shown for both the naive and memory gate.

(C) CCR7 expression, as determined by staining with CCL19-Ig chimera, on naive (solid line) and memory (dotted line) CD8β$^+$ T cells in BM. A histogram for peripheral blood memory CD8$^+$ T cells (dashed line) is shown for comparison. Data are representative of five independent experiments.

(D) Naive and memory subset frequencies among CD8$^+$ T cells in murine and human BM. **$p < 0.01$, ***$p < 0.001$ versus $T_{CM}$s, and ###$p < 0.001$ versus naive T cells ($T_N$s). Error bars show mean ± SEM.

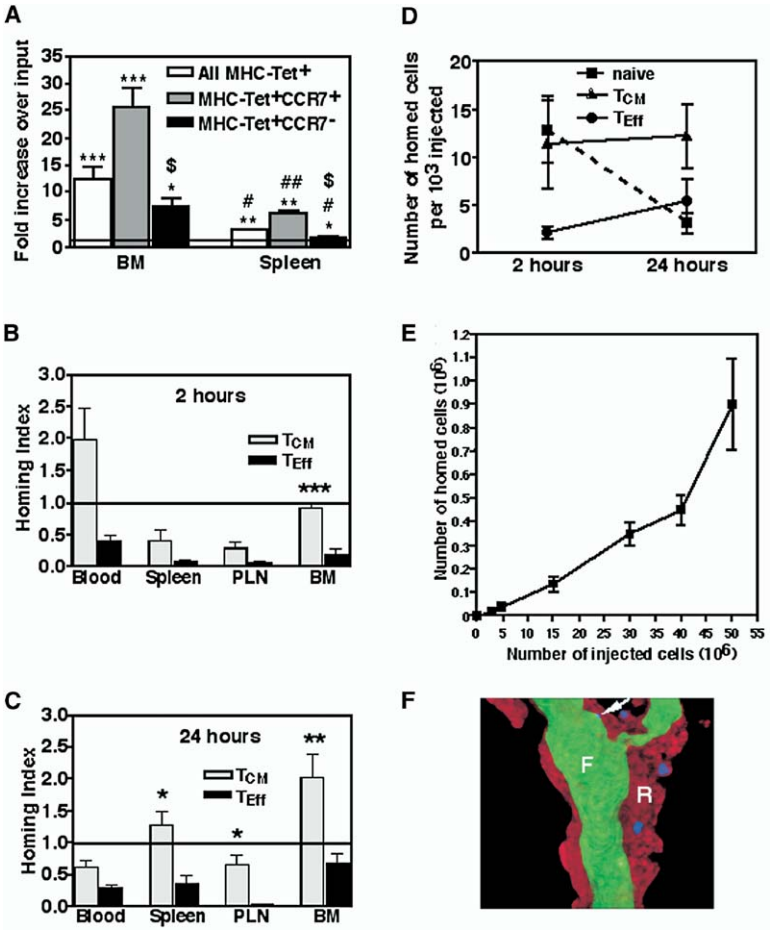


Figure 2. Subset-Specific CD8+ T Cell Homing to the BM

(A) P14 $T_{CM}$s and $T_{EM}$s (CD45.2+) were generated in vivo and injected into CD45.1+ recipients. Frequencies of $T_{CM}$s (MHC-Tet+ CCR7+) and $T_{EM}$s (MHC-Tet+ CCR7−) among CD45.2+ donor cells in BM and spleen were compared with their input frequency. *p < 0.05, **p < 0.01, and ***p < 0.001 versus input. #p < 0.05 and ##p < 0.01 versus corresponding subset in BM (paired Student's t test). $p < 0.05 versus $T_{CM}$s. Error bars show mean ± SEM.

(B and C) Homing of in vitro-generated $T_{CM}$s, $T_{Eff}$s, and naive CD8+ T cells at 2 hr (B) or 24 hr (C) after adoptive transfer. A homing index (HI) of 2 means that Ag-experienced cells were twice as frequent as naive T cells, whereas HI = 1 means that both samples were equivalently represented and so on. Mean ± SEM of at least four mice are shown per group. *p < 0.05, **p < 0.01, and ***p < 0.001 versus HI of $T_{Eff}$s (one-way ANOVA).

(D) Numbers of homed cells recovered from BM at 2 hr and 24 hr after transfer (mean ± SEM).

(E) Dose-response relationship of homed $T_{CM}$s recovered from BM 2 hr after transfer of different numbers of $T_{CM}$s.

(F) Representative 3D projection of optical image stacks obtained by MP-IVM showing homed $T_{CM}$s in murine skull BM. Hoechst 33342-labeled $T_{CM}$s (blue) were injected i.v. 3 hr prior to the recording. The intravascular compartment was delineated by i.v. injection of FITC-dextran (green, "F"). Extravascular hemopoietic tissue was stained with rhodamine 6G (red, "R"). Arrow indicates transmigrating cell. For a 3D video of this scene refer to Movie 1; for a time-lapse video showing $T_{CM}$s migration in BM cavities refer to Movie 2.

duced compared to untreated pathogen-free mice (4.4:1), indicating that mouse BM can harbor substantial numbers of newly generated memory cells other than $T_{CM}$s (Figure S1).

Next, we asked whether the prevalence of $T_{CM}$s in BM could be explained by their migratory properties. Thus, P14 memory cells were generated in vivo as above, and purified T cells (CD45.2+ containing 1.01% tetramer+ cells) were transfused into CD45.1 recipients. 2 hr later, tetramer+ memory cells were markedly enriched among CD45.2+ T cells in recipient spleens and, especially, BM compared to their input frequency (Figure 2A). This effect was mostly due to selective accumulation of $T_{CM}$s, which became 3.5-fold enriched in both tissues compared to $T_{EM}$s. Nevertheless, the tetramer+ $T_{EM}$ concentration in BM was significantly higher than in the input, indicating $T_{EM}$s have enhanced BM tropism, albeit less pronounced than $T_{CM}$s.

To identify the molecular mechanisms of memory CD8+ T cell homing to the BM, much larger numbers of purified memory subsets are needed than for simple homing experiments. Because it is not practical to obtain the required cell numbers from immunized mice, we resorted to in vitro production of $T_{Eff}$s and $T_{CM}$s from naive T cells (Manjunath et al., 2001). We used T-GFP×P14 mice, in which naive T cells and $T_{CM}$s express GFP, and effector CTLs become GFP− (Weninger et al., 2002). Peptide-primed T-GFP×P14 T cells can be differentiated into GFP− $T_{Eff}$s or GFP+ $T_{CM}$-like cells by several days exposure to IL-2 ($CD8^{IL\text{-}2}$) or IL-15 ($CD8^{IL\text{-}15}$), respectively (Manjunath et al., 2001). Their response to recall Ag and ability to migrate to SLOs and inflamed tissue were described previously (Goodarzi et al., 2003; Manjunath et al., 2001; Weninger et al., 2001). In vitro differentiated $CD8^{IL\text{-}2}$ and $CD8^{IL\text{-}15}$ cells are phenotypically similar to endogenous BM-resident $T_{EM}$s and $T_{CM}$s, respectively. This applies to the expression numerous traffic molecules, including CCR7; CXCR4; L-selectin; the integrins CD11a, CD11b, α4, α5, and α4β7; as well as PSGL-1 (Manjunath et al., 2001; Weninger et al., 2001 and data not shown). Thus, $CD8^{IL\text{-}15}$ and $CD8^{IL\text{-}2}$ cells represent faithful surrogates for bona fide $T_{CM}$s and $T_{Eff}$s, respectively, and will be referred to under these names below.

To determine whether in vitro-differentiated $T_{CM}$s and $T_{Eff}$s migrate similarly to memory cells induced in situ, $T_{CM}$s and $T_{Eff}$s were labeled red with TRITC and mixed with T-GFP×P14 splenocytes containing ~30%–35% naive GFP+CD8+ T cells, which served as a reference. Cells were injected into naive mice and the homing index (HI; the ratio of TRITC+:GFP+ naive cells) was deter-

mined in various tissues 2 or 24 hr later. At 2 hr after injection, $T_{CM}$s were most prominent in the blood, whereas naive T cells homed best to SLOs (Figure 2B). $T_{Eff}$s were recovered from all recipient tissues and the blood but at a lower concentration, probably because many of these relatively large blasts were sequestered in lung and liver (Weninger et al., 2001). The BM was the only organ containing equivalent numbers of $T_{CM}$s and naive T cells at 2 hr after injection.

At 24 hr after transfer, the HI of $T_{CM}$s and naive T cells was equivalent in PLN and blood and increased in the spleen, consistent with previous findings (Weninger et al., 2001) (Figure 2C). Although naive T cells were most frequent in the blood, the HI in BM had increased significantly for $T_{CM}$s and, to a lesser degree, also for $T_{Eff}$s. This shift in HI in the BM between 2 and 24 hr is explained by the fact that both naive T cells and $T_{CM}$s were rapidly and efficiently recruited to the BM, but only $T_{CM}$s were retained at this site, whereas naive T cells returned quickly to the circulation (Figure 2D). $T_{Eff}$s homed less well to the BM, but they too were efficiently retained. Thus, our homing experiments are in excellent agreement with our analysis of endogenous BM-resident T cells. Of note, there was a linear relationship between the number of homed and injected $T_{CM}$s (Figure 2E), indicating that homing was not limited by competition with endogenous cells or the BM's capacity to recruit $T_{CM}$s.

### $T_{CM}$ Diapedesis and Migration within BM Cavities

Having determined that $T_{CM}$s possess BM tropism, we focused our further analysis on this subset. First, we employed multiphoton IVM to observe $T_{CM}$s within BM cavities in skulls of anesthetized mice (Mazo et al., 1998). Optical serial sections were rendered as 3D images of BM cavities in which blood vessels were delineated by FITC-dextran (green) and hemopoietic tissue was stained with rhodamine 6G (red). Extravascular $T_{CM}$s carrying blue fluorescence were found within 3 hr after injection (Figure 2F, Movie 1). 3D time-lapse movies showed that the homed $T_{CM}$s were highly motile and migrated at 6.5 ± 0.2 μm/min (mean ± SEM, n = 189 cells), often over long distances (Movie 2). $T_{CM}$ movement was confined to the rhodamine 6G-filled BM cavities and did not occur in adjacent bone but otherwise was random in direction.

### $T_{CM}$s Adhere More Efficiently to BM Microvessels than $T_{Eff}$s

Next, we performed epifluorescence-based video IVM in skull BM (Figure 3). Although this technique does not permit 3D imaging, the fast acquisition rate (30 frames/s) is useful to dissect the molecular mechanisms of rapid adhesion events (Mazo et al., 1998). Fluorescently labeled naive $CD8^+$ T cells, $T_{CM}$s or $T_{Eff}$s were injected into anesthetized mice and their passage through BM microvessels was recorded (Movie 3). $T_{CM}$s rolled ~1.6 times more frequently in BM vessels than $T_{Eff}$s, and the frequency at which rolling cells arrested (sticking fraction) was ~2.2-fold higher (Figure 3A). Consequently, the frequency at which cells entering a microvessel completed the entire multistep adhesion cascade (sticking efficiency) was 3.8-fold higher for $T_{CM}$s than

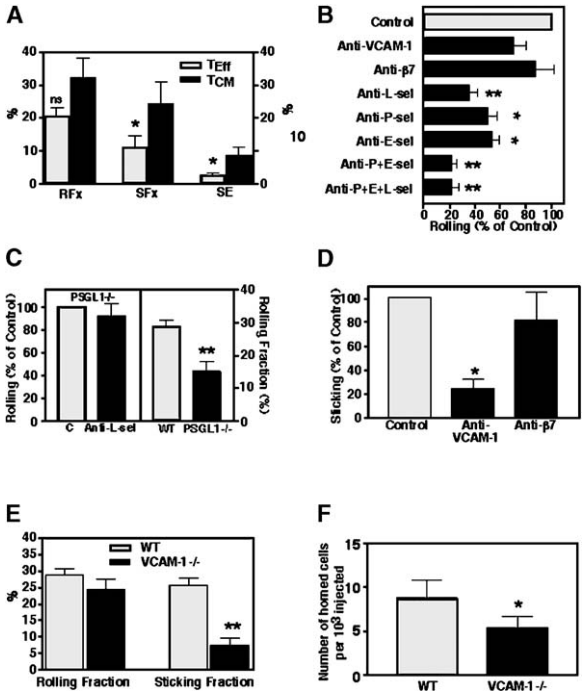


Figure 3. Adhesion Pathways for $T_{CM}$ Homing to BM

(A) $T_{CM}$s display higher intravascular adhesiveness than $T_{Eff}$s. Rolling fractions (RFxs), sticking fractions (SFxs), and sticking efficiencies (SEs) of $T_{CM}$s and $T_{Eff}$s were analyzed in the same microvessels. *$p < 0.05$ versus $T_{CM}$s. Error bars show mean ± SEM.

(B) Effect of mAbs on $T_{CM}$ rolling in BM venules and sinusoids. Results are shown as RFxs after mAb treatment normalized to RFxs in the same vessel prior to mAb injection (control). Error bars show mean ± SEM.

(C) $T_{CM}$ rolling in PSGL-$1^{-/-}$ mice is significantly lower than in wild-type (wt) littermates (right) but is insensitive to anti-L-selectin injection (left). Error bars show mean ± SEM.

(D) Effect of blocking mAbs to VCAM-1 and β7 integrins on $T_{CM}$ sticking in BM microvessels. Error bars show mean ± SEM.

(E) Sticking, but not rolling, of $T_{CM}$s is compromised in VCAM-1 conditional knockout mice. Error bars show mean ± SEM.

(F) $T_{CM}$ homing (24 hr) in VCAM-$1^{-/-}$ mice. Data are presented as mean ± SEM from three to five animals. Results were compared by paired Student's t test (A, C, E, and F) or one-way ANOVA with Bonferroni correction (B and D). *$p < 0.05$, **$p < 0.01$, and ns = not significant versus control or wt. Error bars show mean ± SEM.

$T_{Eff}$s. These findings agree well with our homing experiments and analysis of BM resident memory subsets. Naive T cells underwent rolling and sticking interactions that were similar in frequency to those of $T_{CM}$s (data not shown) and in line with short-term homing experiments (Figure 2B). However, the low frequency of long-term resident naive T cells suggests that additional, as yet unidentified, factors influence the magnitude of steady-state $CD8^+$ T cell subsets in BM.

### Selectins, but Not α4 Integrins, Mediate $T_{CM}$ Rolling in BM Microvessels

Normal BM sinusoids express P- and E-selectin as well as VCAM-1 (Mazo et al., 2002). The latter is a ligand for α4β1 (VLA-4), which mediates stem cell rolling in BM microvessels (Mazo et al., 1998). However, $T_{CM}$ rolling

was normal in BM of wt mice treated with anti-VCAM-1 (Figure 3B) and in mice with a conditional deficiency in endothelial VCAM-1 (Figure 3E). Moreover, $T_{CM}$ treatment with anti-β7 had no effect, indicating that α4β7 is also not involved. By contrast, anti-L-selectin reduced rolling by 64%, whereas mAbs to P- and E-selectin attenuated it by 49% and 46%, respectively (Figure 3B). $T_{CM}$ rolling was also reduced by 48% in mice deficient in PSGL-1, a major selectin ligand (Figure 3C, right). A combination of mAbs to P- and E-selectin blocked additively (by 78%), but there was no further inhibition when anti-L-selectin was added. This suggests that L-selectin mediated secondary tethering whereby endogenous leukocytes adhere to P- and/or E-selectin in BM microvessels and present PSGL-1 as an L-selectin ligand to circulating $T_{CM}$s (Bargatze et al., 1994; Fuhlbrigge et al., 1996; Walcheck et al., 1996). Indeed, anti-L-selectin had no effect on $T_{CM}$ rolling in BM of PSGL-1-deficient mice (Figure 3C, left). Thus, the endothelial selectins in BM microvessels interact with PSGL-1 on circulating $T_{CM}$s, whereas L-selectin on $T_{CM}$s likely contributes indirectly by allowing $T_{CM}$s to tether to other adherent leukocytes.

### The VCAM-1/α4β1 Pathway Mediates $T_{CM}$ Sticking in BM

In most in vivo settings, rolling leukocytes can only arrest by using activation-dependent integrins (von Andrian and Mackay, 2000). Because both the β2 integrin LFA-1 and the α4 integrin VLA-4 are highly expressed on $T_{CM}$s (not shown), we examined these pathways. However, although $T_{CM}$s use LFA-1 to arrest in PLN HEV (Weninger et al., 2001), anti-LFA-1 had no effect on $T_{CM}$ sticking in BM venules or sinusoids (data not shown). By contrast, anti-VCAM-1, the major vascular ligand for VLA-4, reduced $T_{CM}$ sticking by 77% (Figure 3D) and $T_{CM}$ sticking was also 72% lower in conditional VCAM-1 knockout mice than in wt mice (Figure 3E). The importance of VCAM-1 was confirmed in homing experiments; the BM of conditional VCAM-1 knockout mice recruited significantly fewer $T_{CM}$s than wt BM (Figure 3F). However, it is possible that this result reflects not only decreased $T_{CM}$ sticking, because VCAM-1 might also participate in subsequent diapedesis. $T_{CM}$s also express α4β7 (data not shown), which can bind to VCAM-1, but inhibition of this integrin did not affect sticking (Figure 3D). Therefore, VCAM-1–VLA-4 is the principal pathway for $T_{CM}$ arrest in BM microvessels. However, because sticking was not completely abolished without VCAM-1, there is probably at least one additional mechanism for $T_{CM}$ sticking.

### PTX-Sensitive G Protein Signaling Is Required for Optimal $T_{CM}$ Homing, but Not for Integrin Activation in the BM

Integrins support leukocyte sticking only in their high-affinity conformation, which requires activation signal(s) from chemoattractant receptor(s). G protein-coupled receptors (GPCRs), e.g., those for chemokines, can rapidly transmit integrin activation signals. Because most chemoattractant receptors signal through Gαi, they are inhibitable by PTX. Therefore, we performed competitive homing assays comparing differentially labeled, PTX-treated $T_{CM}$s with sham-treated control cells. As expected, 2 hr after injection, significantly fewer PTX-treated $T_{CM}$s had homed to PLN, MLN, and BM, whereas more PTX-treated $T_{CM}$s than untreated cells continued to circulate (HI: 3.4 ± 0.7; Figure 4A). However, although PTX virtually abolished $T_{CM}$ homing to LNs, its effect in the BM was only partial (~60%, inhibition), indicating that Gαi-coupled signals are not absolutely required for $T_{CM}$ lodging in the BM. Results were similar at 24 hr after $T_{CM}$ injection (Figure 4B), except that the difference in circulating cell numbers was less pronounced.

Because homing experiments cannot distinguish between intra- and extravascular $T_{CM}$s in the BM, we asked whether PTX blocked $T_{CM}$ sticking, transmigration, or both. By using 2D epifluorescence and 3D multiphoton IVM, we compared the ability of PTX-treated and control $T_{CM}$s to interact with BM microvessels and to emigrate into BM cavities, respectively. PTX had no significant effect on $T_{CM}$ rolling and, surprisingly, the frequency at which rolling cells arrested was also not different from controls (Figure 5C). By contrast, the fraction of PTX-treated $T_{CM}$s that remained luminally adherent without emigrating was significantly larger than that of control cells (Figure 4C). Consequently, the ratio of extra- to intravascular control $T_{CM}$s was twice as high as that of PTX treated $T_{CM}$s (Figure 4D, Movie 4). Thus, intravascular integrin activation of rolling $T_{CM}$s is independent of Gαi signals, whereas the subsequent diapedesis step depends partially on such signals.

### CXCL12 Induces $T_{CM}$ Sticking, but Not Diapedesis, in BM Microvessels

The chemokine CXCL12 is highly expressed in normal BM (Bleul et al., 1996; Nagasawa et al., 1994). Its receptor CXCR4 is upregulated on memory T cells by IL-15 (Jourdan et al., 2000), and CXCL12 can induce $T_{CM}$ sticking in mouse cremaster muscle venules and PLN HEV (Scimone et al., 2004). Indeed, $T_{CM}$s, but not $T_{Eff}$s, migrated toward a CXCL12 gradient in vitro (Figure 5A). This chemotactic response of $T_{CM}$s was similar to that of naive T cells (not shown) and sensitive to PTX (Figure 5A, inset).

When groups of mice were treated with anti-CXCL12 or an isotype control mAb, $T_{CM}$ homing to the spleen was undisturbed, but homing to the BM of recipients of anti-CXCL12 was significantly reduced (by 37.5%; Figure 5B). Because these results indicated that both PTX and anti-CXCL12 had a similar, if partial, impact on $T_{CM}$ recruitment to the BM, and $T_{CM}$ chemotaxis to CXCL12 was blocked by PTX, it seemed reasonable that the PTX effect was due to inhibition of Gαi signaling via CXCR4. Given our findings with PTX-treated $T_{CM}$s, this hypothesis predicted that CXCL12 should be required for $T_{CM}$ diapedesis, but not for sticking. Surprisingly, IVM experiments with anti-CXCL12 yielded the opposite result. In contrast to PTX, anti-CXCL12 reduced $T_{CM}$ sticking in BM microvessels; the sticking fractions before and after mAb treatment were 38 ± 5% and 21 ± 4%, respectively ($p < 0.01$; Figure 5C). Anti-CXCL12 also reduced the sticking fraction of $T_{CM}$s that had been pretreated with PTX by 47%. Indeed, it ap-

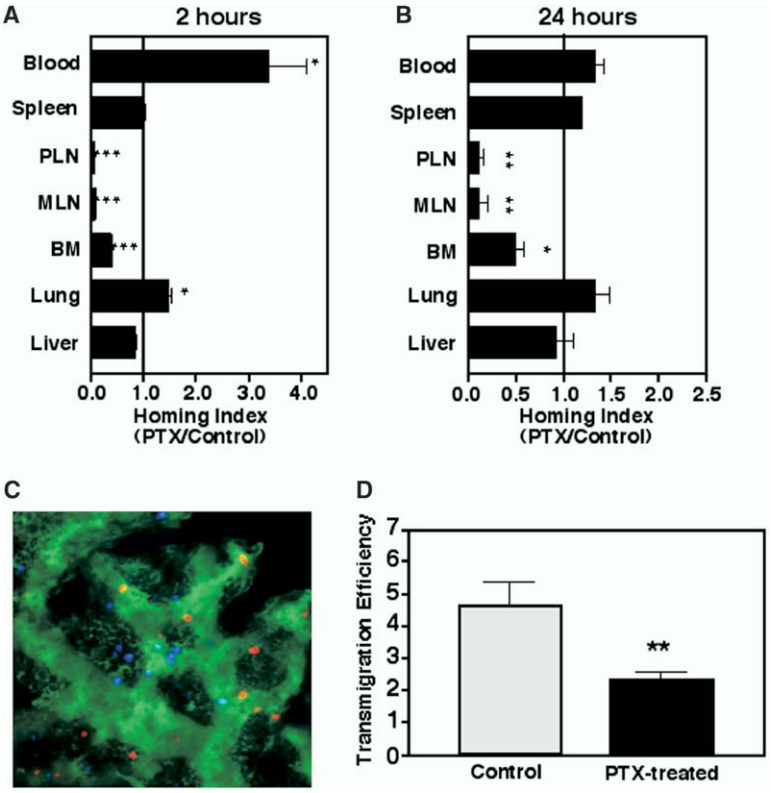


Figure 4. Effect of PTX on $T_{CM}$ Homing and Transmigration

Recipients were sacrificed 2 hr (A) or 24 hr (B) after injection, and homing indices were calculated in indicated organ as ratio of homed PTX-treated cells to control cells (n = 4). Error bars show mean ± SEM.

(C) Representative 3D projection of MP-IVM image stacks demonstrating control (blue) and PTX-treated (red) $T_{CM}$ localization in skull BM 3 hr after injection. Microvessels were contrasted by FITC-dextran (green). A 3D video of this scene is shown in Movie 4.

(D) Transmigration efficiency (ratio of extra- to intravascular cells in the same field of view) of PTX treated and control $T_{CM}$s. Data are from 10 to 12 fields in each of three experiment (mean ± SEM).

Results were compared by one-way ANOVA with Bonferroni correction (A and B) or paired Student's t test (D). *p < 0.05, **p < 0.01, and ***p < 0.001 versus control.

pears that the effect of CXCL12 in $T_{CM}$ traffic to the BM does not at all involve Gαi signaling, because anti-CXCL12, unlike PTX, did not interfere with the ability of sticking $T_{CM}$s to emigrate (Figure 5D).

These results demonstrate that CXCL12 in BM microvessels triggers integrin-dependent, Gαi-independent $T_{CM}$ sticking, but Gαi-coupled signals are required for optimal $T_{CM}$ emigration, which is probably independent of CXCL12. Because sticking and transmigration occur sequentially during BM colonization, interruption of

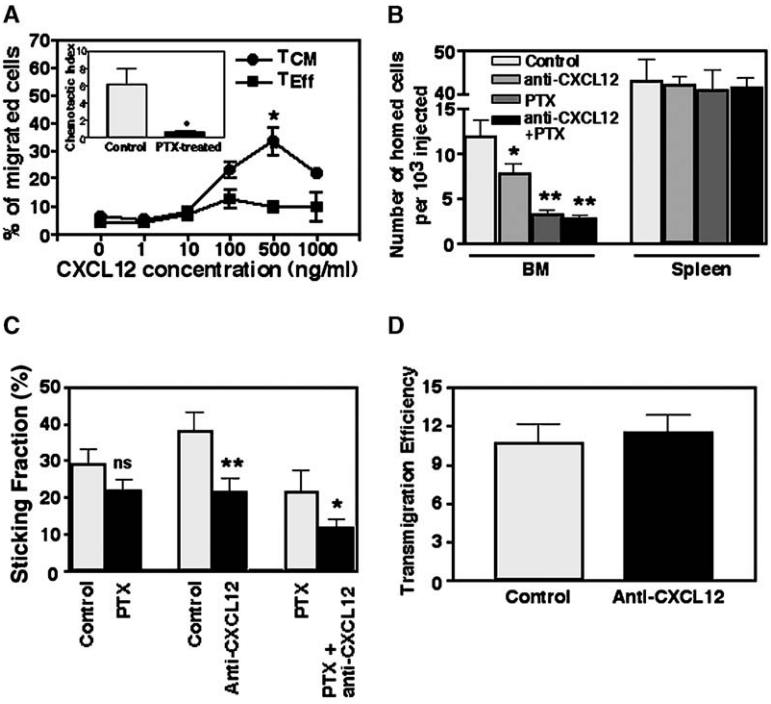


Figure 5. Role of CXCL12 in $T_{CM}$ Homing to BM

(A) $T_{CM}$s possess higher chemotactic activity toward CXCL12 than $T_{Eff}$s. Inset, effect of PTX on $T_{CM}$ migration to 500 ng/ml CXCL12. Error bars show mean ± SEM.

(B) Effect of PTX and anti-CXCL12 on $T_{CM}$ homing to BM and spleen. Error bars show mean ± SEM.

(C) Effect of PTX and anti-CXCL12 on $T_{CM}$ sticking in BM microvessels. Error bars show mean ± SEM.

(D) Transmigration efficiency of $T_{CM}$s across BM microvessels in control and anti-CXCL12-treated mice. Bars represent mean ± SEM from three to five animals. Results were compared by paired Student's t test (A and C) or one-way ANOVA with Bonferroni correction (B). *p < 0.05, **p < 0.01, and ns = not significant.

Table 1. Effect of Differential Treatment with PTX and/or anti-CXCL12 on $T_{CM}$ Sticking, Transmigration Efficiency, and Homing

| Treatment | Sticking (Percentage of Control) | Transmigration (Percentage of Control) | Homing (2 hr) (Percentage of Control) |
|---|---|---|---|
| PTX | 84.1 ± 12.7 | 63.8 ± 8.1** | 30.1 ± 8.0** |
| Anti-CXCL12 | 64.5 ± 16.1* | 108.6 ± 13.7 | 69.1 ± 6.6* |
| PTX+anti-CXCL12 | ND | ND | 25.8 ± 5.3** |

Sticking was determined by 2D epifluorescence IVM, transmigration was determined by 3D MP IVM. *$p < 0.05$, **$p < 0.01$ versus control (paired Student's t test), and ND = no data. Data are presented from four mice.

either step resulted in partially reduced homing of circulating $T_{CM}$s to the BM. However, the effect of Gαi blockade was almost twice as strong as anti-CXCL12, and simultaneous inhibition of both had only a small additive effect (Table 1), suggesting that postadhesion diapedesis is a major rate-limiting event in $T_{CM}$ homing. Nevertheless, even with combination treatment, one quarter of the normal number of $T_{CM}$s continued to access the BM, indicating that additional, as yet unknown mechanism(s) may contribute.

### Adoptively Transferred $T_{CM}$s in Recipient BM Are Long Lived and Mount Potent Recall Responses

Having dissected the multistep adhesion cascade for $T_{CM}$ homing to BM, we asked whether immunocompetent $T_{CM}$s take up long-term residence in the BM. For this, $T_{CM}$s were generated from CD45.2$^+$ OT-IxRAG$^{-/-}$ T cells (which recognize $OVA_{257–264}$ in H-2K$^b$) or P14xTCRα$^{-/-}$ T cells and adoptively transferred to CD45.1$^+$ congenic mice. Recipients were sacrificed 8 weeks later to assess the ability of CD45.2$^+$ T cells in spleen and BM to produce IFN-γ and IL-2 upon rechallenge. In control recipients of naive CD8$^+$ T cells from TCR transgenic mice, the transferred cells became undetectable within 3–5 weeks and no Ag-specific effector activity was detected upon challenge after 8 weeks (data not shown). By contrast, adoptively transferred $T_{CM}$s remained detectable in recipient BM and spleen and readily produced cytokines upon Ag rechallenge, independent on a particular transgenic system used (Figures 6A–6C). No significant cytokine production was observed when T cells were exposed to a control peptide (Figures 6A and 6B).

## Discussion

This study identifies the BM as a major reservoir for CD8 $T_{CM}$s that is equal in size to the splenic $T_{CM}$ pool. $T_{CM}$s are recoverable from BM for months after transfer and potently respond to recall Ag. There are also naive CD8$^+$ T cells and $T_{EM}$s in BM, but these populations are smaller (at least in mice) than naive T cells in SLOs or $T_{EM}$s in spleen, liver, and lung (Weninger et al., 2001). Consistent with the $T_{CM}$-biased composition of BM-resident T cells, both naive T cells and $T_{CM}$s were rapidly recruited to the BM, but only $T_{CM}$s were retained for more than a few hours. In vivo-generated $T_{EM}$s and in vitro-generated $T_{Eff}$s home less well to the BM, presumably because IVM data indicate that they adhere less efficiently to BM vessels. IVM was also used to dissect the multistep cascade for $T_{CM}$ adhesion in BM microvessels and to demonstrate that extravasated $T_{CM}$s migrate vigorously in perivascular BM tissue.

The presence of memory T cells in the BM has been documented previously (Di Rosa and Santoni, 2002, 2003; Kuroda et al., 2000; Marshall et al., 2001; Price and Cerny, 1999; Slifka et al., 1997), and it was also shown that naive and memory T cells home to the BM (Berlin-Rufenach et al., 1999; Di Rosa and Santoni, 2003). The BM can sometimes even function like a SLO where naive T cells can be primed to systemic Ag (Feuerer et al., 2003; Tripp et al., 1997). However, this study represents the first attempt to compare side-by-side the BM tropism of naive and Ag-experienced $T_{CM}$s, $T_{EM}$s, and $T_{Eff}$s with identical antigenic specificity.

To achieve this, we initially used in vivo-generated memory cells to document preferential recruitment of $T_{CM}$s to the BM. We then used a tissue culture approach to produce $T_{Eff}$s and $T_{CM}$s and characterized in detail their adhesive properties in the BM. Culture-derived $T_{CM}$s also allowed us to examine their long-term fate and function. These cytokine-differentiated cells have been extensively characterized previously with regard to surface phenotype, immunological function, mRNA expression profile, and migration in tissues other than the BM (Goodarzi et al., 2003; Manjunath et al., 2001; Ott et al., 2003; Wan et al., 2003; Weninger et al., 2001). Experiments have shown that both in vitro- and in vivo-generated $T_{CM}$s survive after adoptive transfer for several months and mount more potent Ag-specific recall responses than $T_{Eff}$s or $T_{EM}$s (Manjunath et al., 2001; Wherry et al., 2003). However, the anatomical site(s) that shelters $T_{CM}$s has not been identified. Our experiments suggest that the BM is one of these sites.

That $T_{CM}$s possess BM tropism confirms and expands earlier findings that the migratory routes of $T_{CM}$s are distinct from those of other T cells (Sallusto et al., 1999; Scimone et al., 2004; Weninger et al., 2001; Wherry et al., 2003). For example, $T_{CM}$s home to PLN, whereas $T_{Eff}$s fail to accumulate in SLOs other than the spleen (Scimone et al., 2004; Weninger et al., 2001). Conversely, $T_{Eff}$s and $T_{CM}$s are recruited to the liver and inflamed tissues, but naive T cells migrate poorly to these sites (Weninger et al., 2001). However, the BM is the only organ identified to date that emphasizes the recruitment of $T_{CM}$s over all other CD8$^+$ T cells.

To accumulate in tissues, leukocytes undergo a series of adhesive interactions with microvessels that are manifested in tethering, rolling, and sticking (Springer, 1994). Although each adhesion step can be mediated by several receptor-ligand pairs, each leukocyte has at

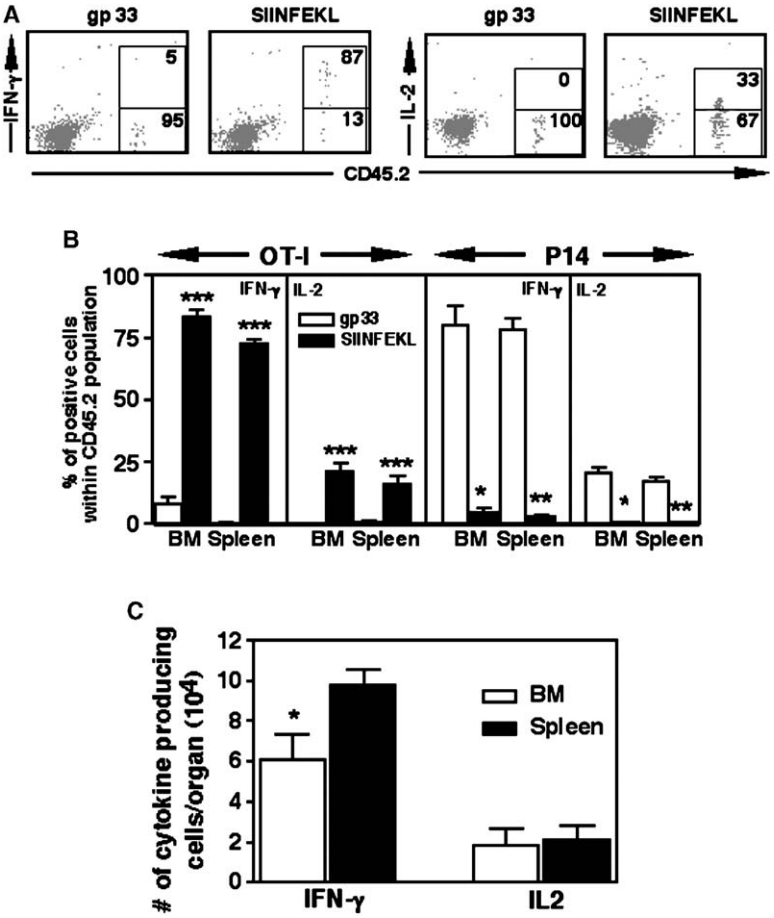


Figure 6. Long-Term Adoptively Transferred $T_{CM}$s in Recipient BM Respond to Recall Ag

(A) Representative dot plots showing intracellular staining of IFN-γ and IL-2 by OT-I $T_{CM}$s in recipient BM 8 weeks after adoptive transfer. $T_{CM}$s responded to cognate peptide (SIINFEKL), but not control gp33. Equivalent results were obtained with P14 $T_{CM}$s (not shown).

(B) Frequency of Ag-specific, cytokine-producing OT-I and P14 $T_{CM}$s harvested from recipient spleens and BM 8 weeks after adoptive transfer. Data were compared with a paired Student's t test. Bars represent mean ± SEM (n = 3). *p < 0.05, **p < 0.01, and ***p < 0.001 versus gp33.

(C) Number of cytokine producing OT-I $T_{CM}$s after stimulation with cognate peptide. *p < 0.05 versus spleen. Error bars show mean ± SEM.

its disposal only a limited, subset-specific set of traffic molecules. Similarly, microvessels in specialized tissues, such as the BM, constitutively express certain traffic molecules, which together specify an anatomically restricted "area code." Only leukocytes whose homing receptor repertoire provides a fit for all adhesion steps have a chance to be recruited. Based on this principle, we can explain the distinct migration patterns of $T_{CM}$s, $T_{Eff}$s and naive $CD8^+$ T cells (Goodarzi et al., 2003; Scimone et al., 2004; Weninger et al., 2001, 2003).

Our IVM study shows that $T_{CM}$ migration to the BM is also a multistep process. This analysis was guided by earlier findings that BM vessels express VCAM-1 as well as P- and E-selectin and that HSC require these molecules for optimal rolling (Mazo et al., 1998, 2002). P/E-selectin also supported $T_{CM}$ rolling but, unlike HSC, $T_{CM}$s did not roll via VCAM-1 but utilized L-selectin, which is not involved in HSC homing to the BM (Mazo et al., 1998). L-selectin did not support direct $T_{CM}$ binding to BM EC but promoted adhesion to PSGL-1 on other adherent leukocytes. This secondary tethering phenomenon has been observed previously in other vascular beds (Eriksson et al., 2001; Sperandio et al., 2003).

Somewhat surprisingly, $T_{CM}$s, but not HSCs, utilized L-selectin, although both cell types are L-selectin$^+$. However, $T_{CM}$s express more L-selectin than the HSCs that were previously studied in our IVM model (I.B.M. and U.H.v.A. unpublished data; Mazo et al., 2002). Indeed, the L-selectin expression level critically determines a leukocyte's ability to interact with endothelial ligands (Gauguet et al., 2004; Sperandio et al., 2001; Tang et al., 1998); Accordingly, the fact that $T_{Eff}$s are L-selectin$^-$ (Manjunath et al., 2001) can explain why more $T_{CM}$s than $T_{Eff}$s roll in BM vessels because only the former can form secondary tethers. Consequently, fewer $T_{CM}$s rolled in BM of PSGL-$1^{-/-}$ than in wt mice. On the other hand, $T_{Eff}$s bind soluble P-selectin-Ig, whereas $T_{CM}$s do not (Manjunath et al., 2001). Nevertheless, $T_{CM}$s rolled in BM via endothelial selectins, indicating that glycoconjugates on $T_{CM}$s can bind surface-expressed selectins in situ, even though they possess insufficient affinity for soluble selectins. Moreover, selectin inhibition probably reduced the number of adherent leukocytes in BM vessels, which may reduce secondary tethering by $T_{CM}$s. Of note, combined inhibition of all selectins did not abolish $T_{CM}$ rolling, indicating that there are additional unidentified rolling pathways.

Our experiments also suggest that an unidentified adhesion receptor(s) contributes to $T_{CM}$ sticking in BM vessels. Unlike in other vascular beds, $T_{CM}$ sticking in BM microvessels was insensitive to anti-LFA-1 and incompletely reduced (by 70%–80%) upon inhibition of α4 integrins or VCAM-1, consistent with previous studies of integrin involvement in lymphocyte homing

to the BM (Berlin-Rufenach et al., 1999; Di Rosa and Santoni, 2002).

Leukocyte integrins, including $\alpha4\beta1$, require a chemoattractant stimulus to undergo arrest. CXCL12 is at least in part responsible for this step in the BM where CXCL12 is physiologically abundant (Bleul et al., 1996; Nagasawa et al., 1994; Peled et al., 1999). $T_{CM}$s express high levels of CXCR4, which triggers $T_{CM}$ sticking in other vascular beds (Scimone et al., 2004). By contrast, $T_{Eff}$s respond poorly to CXL12, presumably because IL-2 downregulates CXCR4 on T cells (Beider et al., 2003). This could explain why few rolling $T_{Eff}$s are arrested in BM vessels. On the other hand, PTX treatment did not reduce $T_{CM}$ sticking in the BM, although it blocks CXCL12-induced adhesion in PLN HEV (Scimone et al., 2004). Similarly, PTX only partially attenuated $T_{CM}$ traffic to the BM but abolished $T_{CM}$ homing to PLN in the same recipients, indicating that the PTX treatment efficiently blocked G$\alpha$i-dependent chemokine signals.

It should be noted that PTX-insensitive sticking in BM microvessels is not unique for $T_{CM}$s, because fetal liver-derived HSCs are also not blocked by PTX (Mazo et al., 2002). CXCR4 can signal through PTX-insensitive G proteins, such as $G_{12}$ or $G_q$ (Kehrl, 1998), which can participate in CXCL12-induced adhesion and migration (Maghazachi, 1997; Soede et al., 2001; Wright et al., 2002). However, only high CXCL12 levels, such as those generated by BM stroma cells, elicit PTX-insensitive T cell responses. CXCL12 requires G$\alpha$i to signal at lower concentrations, as might be prevalent in PLN (Poznansky et al., 2000). Further work will be needed to elucidate why CXCL12 induces G$\alpha$i-independent and G$\alpha$i-dependent $T_{CM}$ arrest in BM and PLN, respectively.

Despite its failure to block sticking, PTX treatment markedly inhibited $T_{CM}$ homing to the BM, presumably by blocking $T_{CM}$ diapedesis. Thus, a G$\alpha$i-dependent chemoattractant that might be distinct from CXCL12 is required for $T_{CM}$ diapedesis. Indeed, BM stromal cells express numerous chemokines (Aman et al., 1993; Broek et al., 2003; Matzer et al., 2001; Tsujimoto et al., 1996; Vanderkerken et al., 2002), and $T_{CM}$s should respond to at least some of them. However, it should be cautioned that CXCL12 has two isoforms, SDF-1$\alpha$ and SDF-1$\beta$ (Tashiro et al., 1993). These splice variants are subject to differential proteolytic processing, tissue distribution, and presentation (De La Luz Sierra et al., 2004). The anti-CXCL12 mAb used here neutralizes SDF-1$\alpha$, but not SDF-1$\beta$. Thus, we cannot exclude that SDF-1$\beta$ contributed to $T_{CM}$ extravasation, whereas SDF-1$\alpha$ (and/or additional chemoattractants) triggered sticking. Indeed, an in vitro study has shown that T cells adhere to activated endothelium after adsorption of CXCL12 (Cinamon et al., 2001); although T cell arrest was PTX-insensitive, subsequent transmigration required CXCL12-induced G$\alpha$i signaling and fluid shear. Still, $T_{CM}$ homing to BM was not abolished when PTX and anti-CXCL12 were combined, thus raising the possibility of an entirely novel recruitment pathway(s). However, without better reagents, it is difficult to rule out that this reflects, at least in part, suboptimal in vivo inhibition of CXCL12, because the mAb used here blocks $T_{CM}$ chemotaxis to CXCL12 by $\leq$85% (data not shown).

What is the benefit of $T_{CM}$ homing to the BM? Memory $CD8^+$ T cells require IL-15 for long-term survival (Ku et al., 2000); the BM may be a rich source for this and other survival factors (Grabstein et al., 1994). Indeed, adoptively transferred $T_{CM}$s established residency in the BM for at least two months. However, this does not necessarily mean that $T_{CM}$s spent this entire time in the BM; there could well be an active steady-state exchange between the BM and other SLOs. Indeed, given that there are substantial numbers of (presumably BM tropic) $T_{CM}$s in the blood (Sallusto et al., 1999; Weninger et al., 2003), we propose that these uniquely immunoprotective T cells use the BM as a major hub, where they find transient shelter before engaging in immunosurveillance elsewhere. This is consistent with a recent study showing rapid turnover of CD8 memory cells in BM of parabiotic mice (Klonowski et al., 2004). However, there could still exist specialized CD8 populations in BM that may not be subject to substantial turnover. For example, the BM is the exclusive residence for a rare subset of $CD8^+CD3\varepsilon^+$ cells that facilitate HSC engraftment after BMT (Schuchert et al., 2000).

The concept that BM-resident $T_{CM}$s are anything but sessile is further suggested by the observation that $T_{CM}$s are constantly moving within BM cavities. Although their migratory velocity was somewhat slower than that of naive T cells in PLN (Mempel et al., 2004; Miller et al., 2003), our findings suggest that $T_{CM}$s in BM can traverse ~400 μm/hr. Unlike in PLN, where T cell migration resembles a random walk (Miller et al., 2003), many $T_{CM}$s in the BM moved preferentially in close proximity and parallel to venules and sinusoids, giving the impression that they were searching for newly extravasated cells. Indeed, in a separate study, we found that circulating DCs migrate to the BM and present Ag to resident $T_{CM}$s (L.L.C., R.B., W.W., I.B.M. and U.H.v.A., unpublished data).

## Experimental Procedures

Mice, mAbs, reagents, tissue culture and chemotaxis methods, homing experiments, and IVM procedures were described previously. Details are provided in the Supplemental Data.

### In Vivo Generation of $T_{CM}$s and $T_{EM}$s

C57Bl/6 donors were implanted with B16 melanoma expressing Flt3 ligand, and splenic DCs were isolated (Opti-Prep, Sigma) 2 weeks later (Mora et al., 2003). Naive T cells were negatively selected (MACS) from spleens and PLN of P14 mice, and $4 \times 10^6$ cells were injected into young adult C57Bl/6 recipients. 24 hr later, the mice were injected i.v. with $10^6$ LPS-matured DCs pulsed with 5 μg/ml gp33-41 peptide (BioSource International). Primed mice were boosted 3 weeks later by injecting $0.5 \times 10^6$ Ag-pulsed DCs. After 5 weeks, Ag-specific P14 memory cells were characterized in BM and spleens by using MHC tetramer H-$2D^b$-PE (Beckman Coulter, Fullerton, CA). Isolated T cells ($2 \times 10^7$ $CD45.2^+$) from SLOs and BM of some immunized mice were transfered to congenic CD45.1 recipients. SLOs and BM were harvested 2 hr later for FACS counting of $CD45.2^+$ MHC tetramer$^+$ $T_{CM}$s and $T_{EM}$s.

### Multiphoton Microscopy

Multiphoton IVM (MP-IVM) was performed with an Olympus BX50 WI microscope, a MaiTai Ti:Sapphire laser (800 nm excitation; Spectra Physics), and a BioRad Radiance 2000MP imaging system. Labeled $T_{CM}$s were detected through bandpass emission filters at 450/80 nm (for Hoechst 33342) or 600/100 nm (for CMTMR). Vessels were visualized after injection of 2 MDa FITC-dextran (525/30

nm filter). The 450/80 nm filter was also used to detect autofluorescence and second harmonic emission from connective tissue. Image stacks were collected at 3–5 μm vertical step size to a depth of 120 μm below the skull surface. For 3D videos, 23 sequential image stacks were acquired at 5 μm z spacing to cover a volume of 210 μm × 210 μm × 110 μm (1 stack/min). Z stacks were processed with Lasersharp (Bio-Rad), Confocal Assistant (freeware), Volocity (Improvision, Coventry, UK), and custom-scripted macros in Adobe Photoshop (Leung, 2002). To assess the role of Gαi in $T_{CM}$ diapedesis, 5 × $10^7$ $T_{CM}$s were treated with PTX, labeled with Hoechst 33342 (5 μg/ml; Sigma), and coinjected i.v. with an equal number of untreated $T_{CM}$s labeled with 10 μM Cell Tracker Orange (CMTMR; Molecular Probes). 3 hr later, mice were prepared for MP-IVM while maintaining the tissue temperature at 37°C by placing a heated circulating water loop and a microthermistor on the skull. Fluorescent dyes were swapped between experiments.

### Cytokine Production

$CD45.2^+$ lymphocytes from spleens and LNs of OT-IxRAG$^{-/-}$ or P14xTCRα$^{-/-}$ donors were differentiated into $T_{CM}$s and 5 × $10^6$ cells injected i.v. into $CD45.1^+$ recipients. 8 weeks later, animals were sacrificed, and single-cell suspensions from recipient spleens and BM were incubated with specific or control peptide (1 μg/ml; 5 hr at 37°C). During the last 2 hr, 1 μM brefeldin A was added, and IFN-γ and IL-2 production of $CD45.2^+$ cells was examined by FACS using a Cytofix/Cytoper kit (PharMingen) and mAbs to IFN-γ and IL-2.

### Statistical Analysis

For comparison of two samples, a two-tailed Student's t test was used. Multiple comparisons were performed by one-way ANOVA with Bonferroni correction. Significance was set at $p < 0.05$. Data in figures and tables are shown as mean ± SEM unless otherwise indicated.

### Supplemental Data

Supplemental Data include Supplemental Experimental Procedures, Supplemental References, one table, one figure, and four movies and can be found with this article online at http://www.immunity.com/cgi/content/full/22/2/259/DC1.

### Acknowledgments

We thank Guiying Cheng and Bruce Reinhardt for technical support, Joe Moore for editorial assistance, and Jean-Marc Gauguet for helpful discussions. This work was supported by National Institutes of Health grants AI061663, HL62524, HL54936, and HL56949 to U.H.v.A. and a T32 grant in Transfusion Medicine from Children's Hospital, Boston (HL66987), the Amy Potter fellowship, and a grant from the Charles Hood Foundation to I.B.M.

Received: June 24, 2004
Revised: January 11, 2005
Accepted: January 12, 2005
Published: February 22, 2005

### References

Adams, G.B., Chabner, K.T., Foxall, R.B., Weibrecht, K.W., Rodrigues, N.P., Dombkowski, D., Fallon, R., Poznansky, M.C., and Scadden, D.T. (2003). Heterologous cells cooperate to augment stem cell migration, homing, and engraftment. Blood *101*, 45–51.

Aman, M.J., Rudolf, G., Goldschmitt, J., Aulitzky, W.E., Lam, C., Huber, C., and Peschel, C. (1993). Type-I interferons are potent inhibitors of interleukin-8 production in hematopoietic and bone marrow stromal cells. Blood *82*, 2371–2378.

Bargatze, R.F., Kurk, S., Butcher, E.C., and Jutila, M.A. (1994). Neutrophils roll on adherent neutrophils bound to cytokine-induced endothelial cells via L-selectin on the rolling cells. J. Exp. Med. *180*, 1785–1792.

Beider, K., Nagler, A., Wald, O., Franitza, S., Dagan-Berger, M., Wald, H., Giladi, H., Brocke, S., Hanna, J., Mandelboim, O., et al. (2003). Involvement of CXCR4 and IL-2 in the homing and retention of human NK and NK T cells to the bone marrow and spleen of NOD/SCID mice. Blood *102*, 1951–1958.

Berlin-Rufenach, C., Otto, F., Mathies, M., Westermann, J., Owen, M.J., Hamann, A., and Hogg, N. (1999). Lymphocyte migration in lymphocyte function-associated antigen (LFA)-1-deficient mice. J. Exp. Med. *189*, 1467–1478.

Bleul, C.C., Fuhlbrigge, R.C., Casasnovas, J.M., Aiuti, A., and Springer, T.A. (1996). A highly efficacious lymphocyte chemoattractant, stromal cell-derived factor 1 (SDF-1). J. Exp. Med. *184*, 1101–1110.

Broek, I.V., Asosingh, K., Vanderkerken, K., Straetmans, N., Van Camp, B., and Van Riet, I. (2003). Chemokine receptor CCR2 is expressed by human multiple myeloma cells and mediates migration to bone marrow stromal cell-produced monocyte chemotactic proteins MCP-1, -2 and -3. Br. J. Cancer *88*, 855–862.

Cinamon, G., Shinder, V., and Alon, R. (2001). Shear forces promote lymphocyte migration across vascular endothelium bearing apical chemokines. Nat. Immunol. *2*, 515–522.

De La Luz Sierra, M., Yang, F., Narazaki, M., Salvucci, O., Davis, D., Yarchoan, R., Zhang, H.H., Fales, H., and Tosato, G. (2004). Differential processing of stromal-derived factor-1alpha and stromal-derived factor-1beta explains functional diversity. Blood *103*, 2452–2459.

Di Rosa, F., and Santoni, A. (2002). Bone marrow CD8 T cells are in a different activation state than those in lymphoid periphery. Eur. J. Immunol. *32*, 1873–1880.

Di Rosa, F., and Santoni, A. (2003). Memory T-cell competition for bone marrow seeding. Immunology *108*, 296–304.

Eriksson, E.E., Xie, X., Werr, J., Thoren, P., and Lindbom, L. (2001). Importance of primary capture and L-selectin-dependent secondary capture in leukocyte accumulation in inflammation and atherosclerosis in vivo. J. Exp. Med. *194*, 205–218.

Feuerer, M., Beckhove, P., Bai, L., Solomayer, E.F., Bastert, G., Diel, I.J., Pedain, C., Oberniedermayr, M., Schirrmacher, V., and Umansky, V. (2001a). Therapy of human tumors in NOD/SCID mice with patient-derived reactivated memory T cells from bone marrow. Nat. Med. *7*, 452–458.

Feuerer, M., Rocha, M., Bai, L., Umansky, V., Solomayer, E.F., Bastert, G., Diel, I.J., and Schirrmacher, V. (2001b). Enrichment of memory T cells and other profound immunological changes in the bone marrow from untreated breast cancer patients. Int. J. Cancer *92*, 96–105.

Feuerer, M., Beckhove, P., Garbi, N., Mahnke, Y., Limmer, A., Hommel, M., Hammerling, G.J., Kyewski, B., Hamann, A., Umansky, V., and Schirrmacher, V. (2003). Bone marrow as a priming site for T-cell responses to blood-borne antigen. Nat. Med. *9*, 151–157.

Fuhlbrigge, R.C., Alon, R., Puri, K.D., Lowe, J.B., and Springer, T.A. (1996). Sialylated, fucosylated ligands for L-selectin expressed on leukocytes mediate tethering and rolling adhesions in physiologic flow conditions. J. Cell Biol. *135*, 837–848.

Gandy, K.L., Domen, J., Aguila, H., and Weissman, I.L. (1999). CD8+TCR+ and CD8+TCR– cells in whole bone marrow facilitate the engraftment of hematopoietic stem cells across allogeneic barriers. Immunity *11*, 579–590.

Garcia-Ojeda, M.E., Dejbakhsh-Jones, S., Weissman, I.L., and Strober, S. (1998). An alternate pathway for T cell development supported by the bone marrow microenvironment: recapitulation of thymic maturation. J. Exp. Med. *187*, 1813–1823.

Gauguet, J.-M., Rosen, S.D., Marth, J.D., and von Andrian, U.H. (2004). Core 2 branching β1,6-N-acetylglucosaminyltransferase and high endothelial cell N-acetylglucosamine-6-sulfotransferase exert differential control over B and T lymphocyte homing to peripheral lymph nodes. Blood *104*, 4104–4112.

Goodarzi, K., Goodarzi, M., Tager, A.M., Luster, A.D., and von Andrian, U.H. (2003). Leukotriene B4 and BLT1 control cytotoxic effector T cell recruitment to inflamed tissues. Nat. Immunol. *4*, 965–973.

Grabstein, K.H., Eisenman, J., Shanebeck, K., Rauch, C., Srinivasan, S., Fung, V., Beers, C., Richardson, J., Schoenborn, M.A., Ahdieh, M., et al. (1994). Cloning of a T cell growth factor that interacts with the beta chain of the interleukin-2 receptor. Science *264*, 965–968.

Hasegawa, H., Nomura, T., Kohno, M., Tateishi, N., Suzuki, Y., Maeda, N., Fujisawa, R., Yoshie, O., and Fujita, S. (2000). Increased chemokine receptor CCR7/EBI1 expression enhances the infiltration of lymphoid organs by adult T-cell leukemia cells. Blood *95*, 30–38.

Jourdan, P., Vendrell, J.P., Huguet, M.F., Segondy, M., Bousquet, J., Pene, J., and Yssel, H. (2000). Cytokines and cell surface molecules independently induce CXCR4 expression on CD4+ CCR7+ human memory T cells. J. Immunol. *165*, 716–724.

Kehrl, J.H. (1998). Heterotrimeric G protein signaling: toles in immune function and fine-tuning by RGS proteins. Immunity *8*, 1–10.

Klonowski, K.D., Williams, K.J., Marzo, A.L., Blair, D.A., Lingenheld, E.G., and Lefrancois, L. (2004). Dynamics of blood-borne CD8 memory T cell migration in vivo. Immunity *20*, 551–562.

Ku, C.C., Murakami, M., Sakamoto, A., Kappler, J., and Marrack, P. (2000). Control of homeostasis of CD8+ memory T cells by opposing cytokines. Science *288*, 675–678.

Kuroda, M.J., Schmitz, J.E., Seth, A., Veazey, R.S., Nickerson, C.E., Lifton, M.A., Dailey, P.J., Forman, M.A., Racz, P., Tenner-Racz, K., and Letvin, N.L. (2000). Simian immunodeficiency virus-specific cytotoxic T lymphocytes and cell-associated viral RNA levels in distinct lymphoid compartments of SIVmac-infected rhesus monkeys. Blood *96*, 1474–1479.

Leung, H. (2002). Photoshop *101*, the sequel: creating XZ images. Bulletin Micros Society Canada *30*, 25–27.

Maghazachi, A.A. (1997). Role of the heterotrimeric G proteins in stromal-derived factor-1alpha-induced natural killer cell chemotaxis and calcium mobilization. Biochem. Biophys. Res. Commun. *236*, 270–274.

Manjunath, N., Shankar, P., Wan, J., Weninger, W., Crowley, M.A., Hieshima, K., Springer, T.A., Fan, X., Shen, H., Lieberman, J., and von Andrian, U.H. (2001). Effector differentiation is not prerequisite for generation of memory cytotoxic T lymphocytes. J. Clin. Invest. *108*, 871–878.

Marshall, D.R., Turner, S.J., Belz, G.T., Wingo, S., Andreansky, S., Sangster, M.Y., Riberdy, J.M., Liu, T., Tan, M., and Doherty, P.C. (2001). Measuring the diaspora for virus-specific CD8+ T cells. Proc. Natl. Acad. Sci. USA *98*, 6313–6318.

Martinez, C., Urbano-Ispizua, A., Rozman, C., Marin, P., Rovira, M., Sierra, J., Montfort, N., Carreras, E., and Montserrat, E. (1999). Immune reconstitution following allogeneic peripheral blood progenitor cell transplantation: comparison of recipients of positive CD34+ selected grafts with recipients of unmanipulated grafts. Exp. Hematol. *27*, 561–568.

Matzer, S.P., Baumann, T., Lukacs, N.W., Rollinghoff, M., and Beuscher, H.U. (2001). Constitutive expression of macrophage-inflammatory protein 2 (MIP-2) mRNA in bone marrow gives rise to peripheral neutrophils with preformed MIP-2 protein. J. Immunol. *167*, 4635–4643.

Mazo, I.B., and von Andrian, U.H. (1999). Adhesion and homing of blood-borne cells in bone marrow microvessels. J. Leukoc. Biol. *66*, 25–32.

Mazo, I.B., Gutierrez-Ramos, J.-C., Frenette, P.S., Hynes, R.O., Wagner, D.D., and von Andrian, U.H. (1998). Hematopoietic progenitor cell rolling in bone marrow microvessels: parallel contributions by endothelial selectins and VCAM-1. J. Exp. Med. *188*, 465–474.

Mazo, I.B., Quackenbush, E.J., Lowe, J.B., and von Andrian, U.H. (2002). Total body irradiation causes profound changes in endothelial traffic molecules for hematopoietic progenitor cell recruitment to bone marrow. Blood *99*, 4182–4191.

Mempel, T.R., Henrickson, S.E., and von Andrian, U.H. (2004). T cell priming by dendritic cells in lymph nodes occurs in three distinct phases. Nature *427*, 154–159.

Miller, M.J., Wei, S.H., Cahalan, M.D., and Parker, I. (2003). Autonomous T cell trafficking examined in vivo with intravital two-photon microscopy. Proc. Natl. Acad. Sci. USA *100*, 2604–2609.

Mora, J.R., Bono, M.R., Manjunath, N., Weninger, W., Cavanagh, L.L., Rosemblatt, M., and von Andrian, U.H. (2003). Selective imprinting of gut-homing T cells by Peyer's patch dendritic cells. Nature *424*, 88–93.

Nagasawa, T., Kikutani, H., and Kishimoto, T. (1994). Molecular cloning and structure of a pre-B-cell growth-stimulating factor. Proc. Natl. Acad. Sci. USA *91*, 2305–2309.

Ott, V.L., Cambier, J.C., Kappler, J., Marrack, P., and Swanson, B.J. (2003). Mast cell-dependent migration of effector CD8+ T cells through production of leukotriene B4. Nat. Immunol. *4*, 974–981.

Peled, A., Grabovsky, V., Habler, L., Sandbank, J., Arenzana-Seisdedos, F., Petit, I., Ben-Hur, H., Lapidot, T., and Alon, R. (1999). The chemokine SDF-1 stimulates integrin-mediated arrest of CD34(+) cells on vascular endothelium under shear flow. J. Clin. Invest. *104*, 1199–1211.

Poznansky, M.C., Olszak, I.T., Foxall, R., Evans, R.H., Luster, A.D., and Scadden, D.T. (2000). Active movement of T cells away from a chemokine. Nat. Med. *6*, 543–548.

Price, P.W., and Cerny, J. (1999). Characterization of CD4+ T cells in mouse bone marrow. I. Increased activated/memory phenotype and altered TCR Vbeta repertoire. Eur. J. Immunol. *29*, 1051–1056.

Sallusto, F., Lenig, D., Forster, R., Lipp, M., and Lanzavecchia, A. (1999). Two subsets of memory T lymphocytes with distinct homing potentials and effector functions. Nature *401*, 708–712.

Schirrmacher, V., Feuerer, M., Fournier, P., Ahlert, T., Umansky, V., and Beckhove, P. (2003). T-cell priming in bone marrow: the potential for long-lasting protective anti-tumor immunity. Trends Mol. Med. *9*, 526–534.

Schuchert, M.J., Wright, R.D., and Colson, Y.L. (2000). Characterization of a newly discovered T-cell receptor beta-chain heterodimer expressed on a CD8+ bone marrow subpopulation that promotes allogeneic stem cell engraftment. Nat. Med. *6*, 904–909.

Scimone, M.L., Felbinger, T.W., Mazo, I.B., Stein, J.V., von Andrian, U.H., and Weninger, W. (2004). CXCL12 mediates CCR7-independent homing of central memory cells, but not naive T cells, in peripheral lymph nodes. J. Exp. Med. *199*, 1113–1120.

Slifka, M., Whitmire, J., and Ahmed, R. (1997). Bone marrow contains virus-specific cytotoxic T lymphocytes. Blood *90*, 2103–2108.

Soede, R.D., Zeelenberg, I.S., Wijnands, Y.M., Kamp, M., and Roos, E. (2001). Stromal cell-derived factor-1-induced LFA-1 activation during in vivo migration of T cell hybridoma cells requires Gq/11, RhoA, and myosin, as well as Gi and Cdc42. J. Immunol. *166*, 4293–4301.

Sperandio, M., Forlow, S.B., Thatte, J., Ellies, L.G., Marth, J.D., and Ley, K. (2001). Differential requirements for core2 glucosaminyltransferase for endothelial L-selectin ligand function in vivo. J. Immunol. *167*, 2268–2274.

Sperandio, M., Smith, M.L., Forlow, S.B., Olson, T.S., Xia, L., McEver, R.P., and Ley, K. (2003). P-selectin Glycoprotein Ligand-1 Mediates L-Selectin-dependent Leukocyte Rolling in Venules. J. Exp. Med. *197*, 1355–1363.

Springer, T.A. (1994). Traffic signals for lymphocyte recirculation and leukocyte emigration: The multi-step paradigm. Cell *76*, 301–314.

Tang, M.L., Steeber, D.A., Zhang, X.Q., and Tedder, T.F. (1998). Intrinsic differences in L-selectin expression levels affect T and B lymphocyte subset-specific recirculation pathways. J. Immunol. *160*, 5113–5121.

Tashiro, K., Tada, H., Heilker, R., Shirozu, M., Nakano, T., and Honjo, T. (1993). Signal sequence trap: A cloning strategy for secreted proteins and type I membrane proteins. Science *261*, 600–603.

Tripp, R.A., Topham, D.J., Watson, S.R., and Doherty, P.C. (1997). Bone marrow can function as a lymphoid organ during a primary immune response under conditions of disrupted lymphocyte trafficking. J. Immunol. *158*, 3716–3720.

Tsark, E.C., Dao, M.A., Wang, X., Weinberg, K., and Nolta, J.A. (2001). IL-7 enhances the responsiveness of human T cells that

develop in the bone marrow of athymic mice. J. Immunol. *166*, 170–181.

Tsujimoto, T., Lisukov, I.A., Huang, N., Mahmoud, M.S., and Kawano, M.M. (1996). Plasma cells induce apoptosis of pre-B cells by interacting with bone marrow stromal cells. Blood *87*, 3375–3383.

Vanderkerken, K., Van de Broek, I., Eizirik, D.L., Van Valckenborgh, E., Asosingh, K., Van Riet, I., and Van Camp, B. (2002). Monocyte chemoattractant protein-1 (MCP-1), secreted by bone marrow endothelial cells, induces chemoattraction of 5T multiple myeloma cells. Clin. Exp. Metastasis *19*, 87–90.

von Andrian, U.H., and Mackay, C.R. (2000). T-cell function and migration. Two sides of the same coin. N. Engl. J. Med. *343*, 1020–1034.

Walcheck, B., Moore, K.L., McEver, R.P., and Kishimoto, T.K. (1996). Neutrophil-neutrophil interactions under hydrodynamic shear stress involve L-selectin and PSGL-1. A mechanism that amplifies initial leukocyte accumulation of P-selectin in vitro. J. Clin. Invest. *98*, 1081–1087.

Wan, J., Martinvalet, D., Ji, X., Lois, C., Kaech, S.M., von Andrian, U.H., Lieberman, J., Ahmed, R., and Manjunath, N. (2003). The Bcl-2 family pro-apoptotic molecule, BNIP3 regulates activation-induced cell death of effector cytotoxic T lymphocytes. Immunology *110*, 10–17.

Weninger, W., Crowley, M.A., Manjunath, N., and von Andrian, U.H. (2001). Migratory properties of naive, effector, and memory CD8(+) T cells. J. Exp. Med. *194*, 953–966.

Weninger, W., Manjunath, N., and von Andrian, U.H. (2002). Migration and differentiation of CD8+ T cells. Immunol. Rev. *185*, 221–233.

Weninger, W., Carlsen, H.S., Goodarzi, M., Moazed, F., Crowley, M.A., Baekkevold, E.S., Cavanagh, L.L., and von Andrian, U.H. (2003). Naive T cell recruitment to non-lymphoid tissues: a role for endothelium-expressed CCL21 in autoimmune disease and lymphoid neogenesis. J. Immunol. *170*, 4638–4648.

Wherry, E.J., Teichgraber, V., Becker, T.C., Masopust, D., Kaech, S.M., Antia, R., von Andrian, U.H., and Ahmed, R. (2003). Lineage relationship and protective immunity of memory CD8 T cell subsets. Nat. Immunol. *4*, 225–234.

Wright, D.E., Wagers, A.J., Gulati, A.P., Johnson, F.L., and Weissman, I.L. (2001). Physiological migration of hematopoietic stem and progenitor cells. Science *294*, 1933–1936.

Wright, N., Hidalgo, A., Rodriguez-Frade, J.M., Soriano, S.F., Mellado, M., Parmo-Cabanas, M., Briskin, M.J., and Teixido, J. (2002). The chemokine stromal cell-derived factor-1 alpha modulates alpha 4 beta 7 integrin-mediated lymphocyte adhesion to mucosal addressin cell adhesion molecule-1 and fibronectin. J. Immunol. *168*, 5268–5277.

Zeng, D., Hoffmann, P., Lan, F., Huie, P., Higgins, J., and Strober, S. (2002). Unique patterns of surface receptors, cytokine secretion, and immune functions distinguish T cells in the bone marrow from those in the periphery: impact on allogeneic bone marrow transplantation. Blood *99*, 1449–1457.